



# Fault Analysis of Three-Level NPC Inverters in Synchronous Reluctance Motor Drives

Diogo B. Matos, Jorge O. Estima, Antonio Marques Cardoso

## ► To cite this version:

Diogo B. Matos, Jorge O. Estima, Antonio Marques Cardoso. Fault Analysis of Three-Level NPC Inverters in Synchronous Reluctance Motor Drives. 7th Doctoral Conference on Computing, Electrical and Industrial Systems (DoCEIS), Apr 2016, Costa de Caparica, Portugal. pp.206-216, 10.1007/978-3-319-31165-4\_21 . hal-01438246

**HAL Id: hal-01438246**

**<https://inria.hal.science/hal-01438246>**

Submitted on 17 Jan 2017

**HAL** is a multi-disciplinary open access archive for the deposit and dissemination of scientific research documents, whether they are published or not. The documents may come from teaching and research institutions in France or abroad, or from public or private research centers.

L'archive ouverte pluridisciplinaire **HAL**, est destinée au dépôt et à la diffusion de documents scientifiques de niveau recherche, publiés ou non, émanant des établissements d'enseignement et de recherche français ou étrangers, des laboratoires publics ou privés.



Distributed under a Creative Commons Attribution 4.0 International License

# Fault Analysis of Three-Level NPC Inverters in Synchronous Reluctance Motor Drives

Diogo M. B. Matos<sup>1</sup>, Jorge O. Estima<sup>1</sup>, and Antonio J. Marques Cardoso<sup>1</sup>

<sup>1</sup> CISE – Electromechatronic Systems Research Centre, University of Beira Interior,  
Covilhã, Portugal  
cise@ubi.pt

**Abstract.** A performance analysis of a synchronous reluctance motor (SynRM) drive, operating under different fault conditions, with a three-level NPC inverter, controlled by a seven-segment Space Vector Modulation (SVM) technique, is presented in this paper. Considering the voltage source inverter, open-circuit faults of different types are introduced and their effects are studied regarding the SynRM and the inverter performance evaluation. The healthy and faulty operating conditions comparison will take into account the evaluation of some variables, such as the motor power factor, electromagnetic torque, efficiency, total waveform distortion values, currents RMS values, and total waveform oscillation values, obtained from simulation results.

**Keywords:** Open-circuit faults, synchronous reluctance motor, inverter failures, three-level NPC inverter failures.

## 1 Introduction

During the last years, the interest in the use of synchronous reluctance motors (SynRMs) has increased quite a lot due to their high efficiency, simple structure and rugged characteristics. Moreover, these motors are capable to operate in high-speed applications and in high-temperature environments, enhancing their potential for high-performance variable speed drives [1], [2], [3], [4].

Likewise, there has been a growing use of multilevel inverters (MI) such as the neutral point clamped (NPC) converters, since comparing with the traditional two-level converters, they provide higher output voltage waveform quality, lower harmonic content, lower  $dv/dt$  transients and lower switching losses. In addition, due to the availability of more voltage levels, switching-states or voltage-levels redundancy, and space vectors redundancy, actually, these converters are used in many critical applications in which it is necessary to maximize the reliability of the system through fault-tolerant capability [5], [6], [7]. Note also that, traditionally, the use of MI has been associated to high- and medium-voltage applications, whereas, nowadays, it is known that its use is also viable for low-power and low-voltage applications [8], [9]. Despite all that, it is worth mentioning that the more complex structure associated to the MIs may result also in additional problems which do not occur with traditional converters. The MIs comprise a greater number of components

that result in higher costs. At the same time, the increase of the semiconductors may result in a reduction of the reliability of the system, since a failure in a semiconductor device may cause severe damages on the drive system. In general, power device failures can be classified as open-circuit faults and short-circuit faults. Typically, short-circuit faults are more destructive, requiring special care. Open-circuit faults do not necessarily cause the system shutdown and can remain undetected for an extended period of time. This may lead to secondary faults in the converter or in the remaining drive components, resulting in the total system shutdown and high repairing costs. Moreover, in the particular case of the NPC inverter, issues related to the unbalanced voltage of the dc-link capacitors must be also addressed. Depending on the operating conditions, different voltages values at the capacitors' terminals may occur, which cause undesirable distortion at the inverter output [5], [7].

Several studies have been presented regarding to the most diverse aspects related to the NPC inverters. On one hand, issues related to the capacitors voltage unbalance in some operating conditions has been addressed in [5], [7], [10], [11], [12], assuming nowadays as a solved problem. On the other hand, subjects such as control techniques and fault-tolerant solutions have also been addressed, observing significant contributions in these fields in the last years [13], [14], [15], [16]. Regarding the fault-tolerant capability, this topic is particularly interesting for NPC inverters, since it is considered that NPC converters present limited fault tolerance.

Although many studies have been published on these fields, few studies exist with respect to what happens after the occurrence of a failure. Besides, usually the analyses are carry out mainly for PMSM drives and induction motor drives operating under faulty conditions, being provided much less attention to the SynRM performance under the same conditions. Hence, some of these issues are discussed in this paper when semiconductor open-circuit faults occur. These faults are introduced in a three-level NPC converter, controlled by a SVM technique, allowing the control of the machine speed. The SynRM performance assessment will take into account the evaluation of some variables, such as the motor power factor, electromagnetic torque, efficiency, total waveform distortion (TWD) values, currents RMS values, and total waveform oscillation values (TWO), obtained from simulation results.

## 2 Relationship to Cyber-Physical Systems

Cyber-Physical Systems (CPS) is a new concept that has been developed in recent years as a result of the integration of computer systems, networking and physical processes. It is expected that the advances in the CPS will enable capability, adaptability, scalability, resiliency, safety, security, and usability, which will exceed widely the embedded systems of today.

By definition, CPS are related to the integration of computation, networking and the control of physical processes, where physical processes affect computations and vice versa. In this context, electric drives as the one presented in this work, can be easily integrated in a CPS. These applications are strictly related to the control of physical processes, which is a fundamental part of a CPS. Moreover, nowadays, CPS based on electric drives are widely used in industry. Some examples can be pointed

out, such as the case of electric power plants and complex transformation industries, where a great number of electric drives are connected to a monitoring network, providing constant data exchange to a main computational platform, allowing for precise control and monitoring of the entire production/transformation processes.

### 3 SynRM Model

The SynRM model  $dq$  equivalent circuits, including iron losses and saturation in the synchronous reference frame, are presented in Fig. 1. An extra resistor  $R_c$  connected in parallel with the magnetizing branch in both  $d$  and  $q$  axes is used to take into account the iron losses effect.

The effect of magnetic saturation was also considered in the SynRM model by modeling the  $d$  and  $q$  axes inductances as dependent on the supply current. It is worth noting that the saturation effect in the  $d$  axis will be distinct from the one in the  $q$  axis, since the magnetic paths around the rotor present different reluctances. For this reason,  $dq$  axes saturation behavior will be different with the current variation.

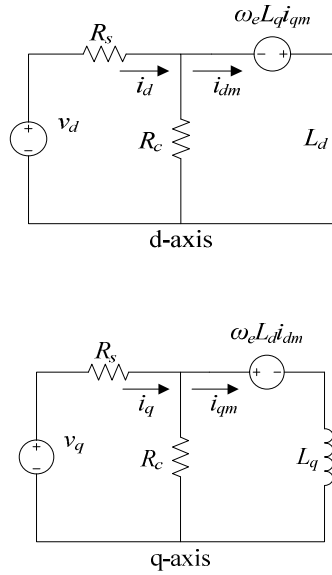


**Fig. 1.** SynRM  $dq$  equivalent circuits in the synchronous reference frame.

Taking this into account, the SynRM voltage equations in the synchronous reference frame are expressed by:

$$v_d = R_s i_d - \omega_e L_q i_{qm} + L_d \frac{di_d}{dt} \quad (1)$$

$$v_q = R_s i_q - \omega_e L_d i_{dm} + L_q \frac{di_{qm}}{dt} \quad (2)$$

where  $i_d$  and  $i_q$  are the  $dq$  axes supply currents,  $v_d$  and  $v_q$  are the  $dq$  axes supply voltage components,  $i_{dm}$  and  $i_{qm}$  are the  $dq$  axes magnetizing currents,  $L_d$  and  $L_q$  are the  $dq$  axes inductance components (which depend on the  $i_{dm}$  and  $i_{qm}$  currents),  $R_c$  and  $R_s$  are the iron losses resistance and the stator resistance, and finally,  $\omega_e$  represents the electrical frequency. The electromagnetic torque expression and the mechanical moving equation are given by:

$$T_e = \frac{3}{2} p (L_d - L_q) i_{dm} i_{qm} \quad (3)$$

$$T_e = J \frac{d\omega_m}{dt} + B_m \omega_m + T_L + T_k \quad (4)$$

where  $T_e$  is the developed electromagnetic torque,  $p$  the number of pole pairs,  $T_L$  is the load torque,  $J$  represents the system moment of inertia,  $B_m$  is the viscous friction coefficient,  $\omega_m$  is the mechanical speed of the motor and  $T_k$  is the constant friction coefficient.

#### 4 Control of Three-Level NPC Inverter

The power circuit of the three-level NPC inverter is shown in the Fig. 2. Each inverter leg is composed of four IGBT switches ( $S_{x1}$  to  $S_{x4}$ , where  $x=a,b,c$ ) with antiparallel diodes, and two clamping diodes ( $D_{x1}$  and  $D_{x2}$ ), which are connected between the pairs of upper and lower IGBT switches ( $S_{x1}/S_{x2}$  and  $S_{x3}/S_{x4}$ ) and the middle point  $O$ . The middle point is available since on the DC side of the inverter, the DC bus capacitor is split into two. Note, however, that the correct neutral point potential at the middle point  $O$  is only achieved if the capacitor voltages are balanced.

The operating states of the switches in each NPC inverter leg can be characterized by the three switching states shown in Table 1. The switching state  $P$  indicates that the upper two switches of the leg  $x$  are turned on and the inverter terminal voltage  $V_{x0}$  is  $+V_{dc}/2$ . In contrast, the switching state  $N$  means that the two lower semiconductor devices are turned on, leading to a  $V_{x0}$  value equal to  $-V_{dc}/2$ . In turn, the switching state  $O$  signifies that the two inner switches are turned on, and therefore,  $V_{x0}$  is connected to the middle point through the clamping diodes. In an ideal operating condition this means that  $V_{x0}$  is equal to zero.

Regarding the control, only a good sequence of switching states enables a suitable operation of the drive. This implies an appropriate selection of the reference vector  $\vec{V}_{ref}$ , in order to be generated just the required voltage for the operation of the

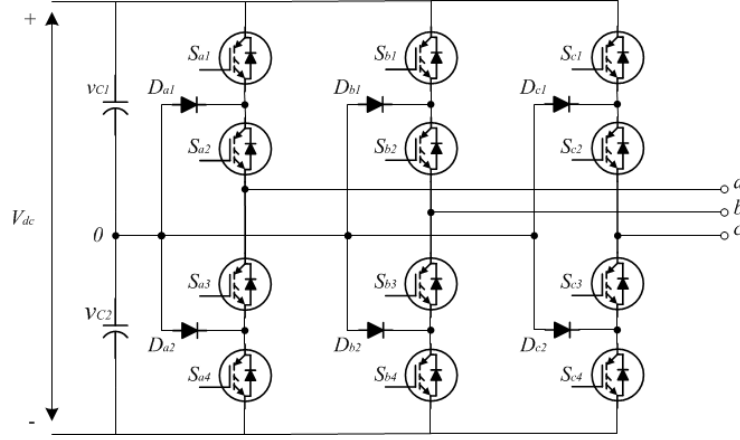


**Fig. 2.** Circuit diagram of three-level neutral-point clamped inverter.

**Table 1.** Definition of the NPC converter switching states.

Switching State	Device Switching Status				Inverter Terminal Voltage $V_{x0}$
	$S_{x1}$	$S_{x2}$	$S_{x3}$	$S_{x4}$	
P	On	On	Off	Off	$+V_{dc}/2$
O	Off	On	On	Off	0
N	Off	Off	On	On	$-V_{dc}/2$

Considering the switching states  $P$ ,  $O$ , and  $N$  for each leg, the inverter has  $3^3 = 27$  different switching state combinations that result in the voltage vectors distribution throughout a space vector diagram, as shown in Fig. 2. Some of the switching states are redundant, since they generate the same voltage vector.

The SVM technique will modulate the reference vector using the three nearest vectors, based on the “volt-second balancing” principle [17]. In order to accomplish this, the modulator needs to know the position of the reference voltage vector on the space vector diagram to identify the closest vectors.

In the present work, a seven-segment SVM scheme was used. An overview of the applied SVM control is shown in Fig. 3. As it can be seen, first, it is identified the region, sector and the modulation index related to the reference vector needed for the SynRM operation. After that, it is calculated the dwell times for the application of vectors considering the modulation period  $T_s$ . Lastly, it is used a lookup table to generate the switching states based on the calculated above.

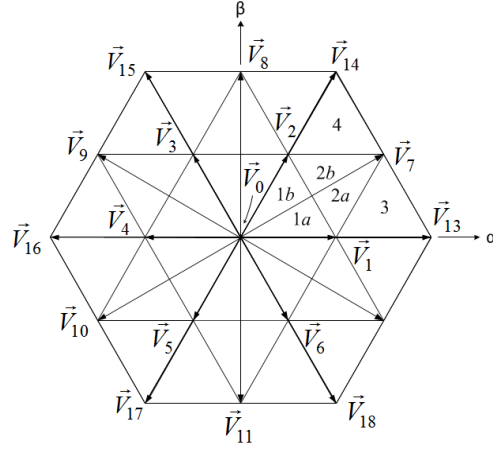


**Fig. 3** Space vector diagram of the NPC inverter.

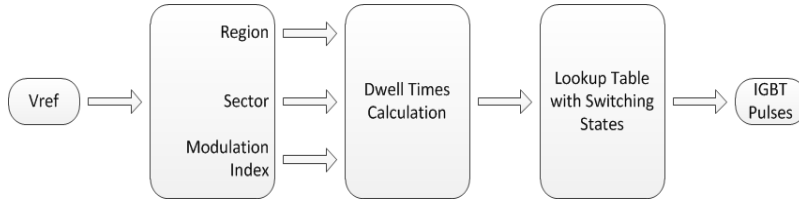


**Fig. 4** Schematic diagram of the implemented SVM technique.

## 5 Simulation Results

The MATLAB/Simulink programming language was used for the modeling and simulation of the SynRM variable speed drive. The machine mathematical model was connected to a three-level NPC power converter controlled by a SVM rotor field oriented control algorithm.

The SynRM performance was assessed by considering three distinct operating modes: normal operation conditions, an inverter single semiconductor open-circuit failure in IGBT  $S_{a1}$  and in IGBT  $S_{a2}$ .

The SynRM phase currents evaluation was performed by calculating of the RMS and the total waveform distortion (TWD) values. The TWD coefficient expresses the SynRM currents' harmonic content and it is given by:

$$TWD = \frac{\sqrt{I_{RMS}^2 - I_1^2}}{I_1} \times 100\% \quad (5)$$

where  $I_{RMS}$  and  $I_1$  represent the current's total RMS value and the fundamental component RMS value, respectively. In turn, the analysis of the electromagnetic torque was performed by obtaining the Total Waveform Oscillation (TWO) factor, which is directly related to the amount of the torque ripple:

$$TWO = \frac{\sqrt{T_{eRMS}^2 - T_{eDC}^2}}{|T_{eDC}|} \times 100\% \quad (6)$$

where  $T_{eRMS}$  and  $T_{eDC}$  are the RMS and mean values of the electromagnetic torque, respectively. Other computational simulations were performed in order to obtain the motor power factor (PF) and efficiency ( $\eta$ ) for the different considered operating conditions.

The evaluation and comparison of all considered operating conditions was performed for the same values of speed and torque. A reference speed of 1200 rpm was assumed together with a constant load torque that was equivalent to the SynRM rated value. In Table 2 are presented the SynRM parameters used in this study.

**Table 2.** SynRM dataplate parameters.

Parameters	Values
<i>Power</i>	2.2 kW
<i>Voltage</i>	400 V
<i>Current</i>	5.69 A
<i>Speed</i>	1500 rpm
<i>N° of pole pairs</i>	2
<i>Moment of inertia</i>	0.0018 kg.m <sup>2</sup>

### 5.1 Normal Operating Conditions

The SynRM phase *a* current and electromagnetic torque spectrograms and their corresponding time-domain waveforms under normal operating conditions are shown in Fig. 5. (a) and (b).



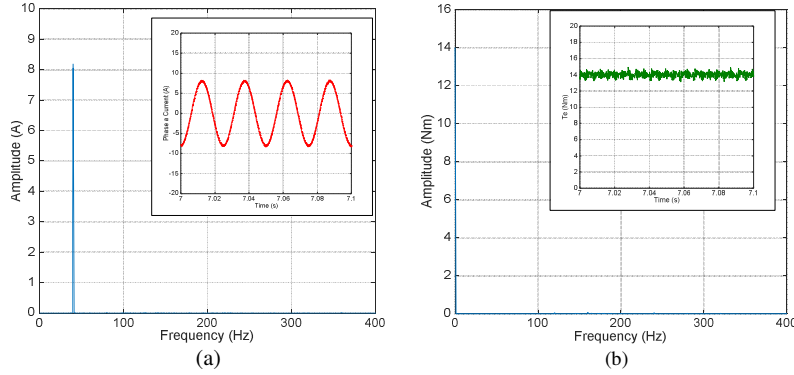


**Fig. 5.** Spectrogram and time-domain waveform of the SynRM: (a) phase  $a$  current; (b) electromagnetic torque (under normal operating conditions).

As it can be seen, the SynRM phase currents are virtually sinusoidal, presenting low noise and a well-defined fundamental component. As a result, a TWD value equal to 1.59% together with a RMS value of 5.69 A were obtained for each motor phase.

Regarding the SynRM electromagnetic torque, it can be observed that it presents only low amplitude high-frequency noise and that it is basically constant, resulting in a low TWO value equal to 1.97%.

As far as the motor efficiency and power factor is concerned, the values of 89.67% and 0.684, were, respectively, obtained.

## 5.2 Single Semiconductor Open-Circuit Failure in IGBT $S_{a1}$ /IGBT $S_{a2}$

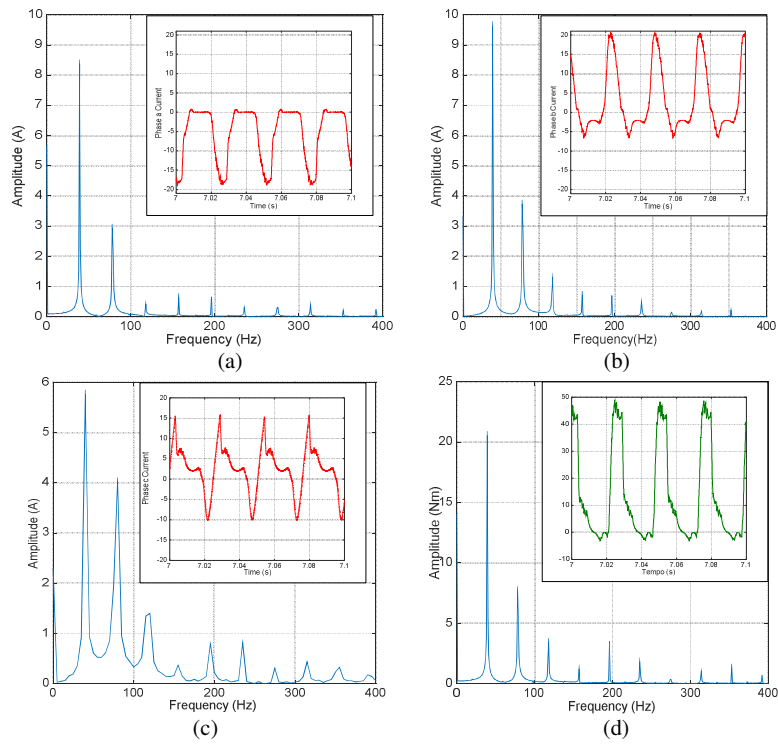
With the aim to introduce semiconductor single open-circuit faults, the corresponding gate signals for the IGBT were set to zero. It is worth noting that in both cases the antiparallel diode remains connected. Furthermore, several simulations were performed and it was concluded that for these specific operating conditions, the failures in IGBT  $S_{a1}$  or IGBT  $S_{a2}$  result in very similar effects. Thus, the results will be presented for only one of these situations (fault in IGBT  $S_{a1}$ ). The failures also lead to the discharge of the lower capacitor and, conversely, a charge of the upper capacitor to a value approximately twice of the initial one, which results in the loss of the three voltage levels and, at the same time, an overvoltage of healthy semiconductors.

Under these faulty conditions, the NPC power converter becomes unbalanced, resulting in different current waveforms. Fig. 6 a), b), and c) show these waveforms together with the corresponding spectrogram. Analyzing the data, it can be easily observed that the machine phase currents present a very distorted waveform. Consequently, the TWD values increase considerably, as shown in Table 3. Moreover the SynRM losses are negatively affected due to the existence of a large DC component and a high second order harmonic.

**Table 3.** RMS and TWD values for an inverter failure in IGBT  $S_{a1}$ .

Parameters	Phase $a$	Phase $b$	Phase $c$
RMS (A)	9.04	9.04	6.13
TWD (%)	100.73	70.75	109.02

By analyzing the RMS values, it can be also concluded that the NPC converter is operating under unbalanced conditions. Since the power switch IGBT  $S_{a1}$  is opened, and considering the system steady-state operation after the failure, the phase  $a$  current cannot assume positive values.

**Fig. 6.** Spectrogram and time-domain waveform of the SynRM: (a) phase  $a$  current; (b) phase  $b$  current; (c) phase  $c$  current; (d) electromagnetic torque (for an open-circuit fault in IGBT T1).

The SynRM electromagnetic torque waveform together with its corresponding spectral analysis is depicted in Fig. 6(d). These results demonstrate that the electromagnetic torque presents a strong oscillation/ripple. Contrary to the results obtained for the healthy case, the electromagnetic torque is not smooth anymore,

being clearly visible high frequency harmonic components multiple of the fundamental frequency, resulting in a TWO value of 130.32%. This fact proves that under these operating conditions, the SynRM shaft suffers strong mechanical efforts which may endanger the drive operation.

Regarding the machine efficiency and power factor, the values of 81.77% and 0.436, were, respectively, obtained for this specific operating mode. Due to the increase of RMS values, the copper losses are also higher, resulting in a large SynRM input power and lower efficiency. On the other hand, under these circumstances the machine apparent power is also increased, resulting in a low power factor value.

## 6 Experimental Implementation Plan

Currently, further work is being carried out in order to build the setup for the experimental validation. A 2.2 kW 1500 rpm SynRM with similar characteristics to the one used in the simulation results will be used. A Semikron three-level NPN converter will be acquired, which already includes the power switch modules and their corresponding drive circuits and protections. The drive control algorithm will be implemented into a dSPACE DS1103 system. An incremental encoder with a resolution of 2048 pulses per turn will be used to measure the motor shaft position. The dSPACE platform provides a dedicated software that allows to build a real-time user interface that can be used to introduce converter faults by disabling the semiconductors gate pulses.

## 7 Conclusions

This paper has presented a performance evaluation of a SynRM variable speed drive fed by a three-level NPC converter under distinct faulty conditions. The drive healthy operation was assessed as well as the case where power converter open-circuit failures in IGBT Sa1 and IGBT Sa2 were considered. The SynRM performance assessment was based on the evaluation of some variables like the motor power factor, electromagnetic torque, efficiency, TWD, currents RMS values, and TWO values.

It has been concluded that when the three-level NPC converter presents a single semiconductor open-circuit failure, the SynRM supply currents will be negatively affected due to their large harmonic distortion. As a consequence, there is a noticeable increase of their TWD values, being observed a strong electromagnetic torque pulsating waveform. The motor efficiency and power factor are also reduced due to the increase of the RMS values of the two remaining healthy phases.

As future work, the analysis of the distinct patterns and behavior of the different variables under these abnormal operating conditions will enable the development of appropriate fault diagnostic techniques. Finally, after identifying the damaged devices, fault-tolerant remedial strategies can be then implemented in order to improve the drive's performance.

**Acknowledgment.** The authors acknowledge the financial support from the Portuguese Foundation for Science and Technology (FCT) under grant nº SFRH/BD/102345/2014 and grant nº SFRH/BPD/87135/2012.

## References

1. Lipo, T. A.: Synchronous Reluctance Machines – A viable alternative for ac drives?. In: Electric Machines and Power Systems, vol. 19, pp 659–671 (1991)
2. Yahia, K., Matos, D. M. B., Estima, J. O., Cardoso, A. J. M.: Modeling Synchronous Reluctance Motors Including Saturation, Iron Losses and Mechanical Losses. In: Proceedings of the 22nd International Symposium on Power Electronics, Electrical Drives, Automation and Motion, pp. 595–600. Ischia, Italy (2014)
3. Matos, D. M. B., Estima, J. O., Yahia, K., Cardoso, A. J. M.: Modeling and Implementation of MTPA Control Strategy for SynRM Variable Speed Drives. In: International Review of Electrical Engineering, vol.9, no. 6 (2014)
4. Matos, D. M. B. Estima, J. O., Cardoso, A. J. M.: Performance Evaluation of Synchronous Reluctance Motor Drives under Inverter Fault Conditions. In: 10<sup>th</sup> IEEE International Symposium on Diagnostics for Electric Machines, Power Electronics and Drives. Guarda (2015)
5. Franquelo, L.G., Rodríguez, J., León, J.I., Kouro, S., Portillo, R., and Prats, M.M.: The age of multilevel converters arrives. In: IEEE Industrial Electronic Magazine, vol. 2, no. 2, pp. 28–39 (2008)
6. Rodríguez, J., Bernet, S., Steimer, P.K., and Lizama, I.E.: A survey on neutral-point-clamped inverters. In: IEEE Transactions on Industrial Electronics, vol. 57, no. 7, pp. 2219–2230 (2010)
7. Abu-Rub, H., Holtz, J., Rodriguez, J., and Baoming, G.: Medium voltage multilevel converters – State of the art, challenges and requirements in industrial applications. In: IEEE Transactions on Industrial Electronics, vol. 57, no. 8, pp.2581–2596 (2010)
8. Teichmann, R., Malinowski, M., and Bernet, S.: Evaluation of three-level rectifiers for low-voltage utility applications. In IEEE Transactions on Industrial Electronics, vol. 52, no. 2, pp. 471–481 (2005)
9. Teichmann, R., and Bernet, S.: A comparison of three-level converters versus two-level converters for low-voltage drives, traction, and utility applications. In: IEEE Transactions on Industrial Applications, vol. 42, no. 3, pp. 855–865 (2005)
10. Lin, L., Zou, Y., Wang, Z., and Jin, H.: Modeling and control of neutral point voltage balancing problem in three-level NPC PWM inverters. In: Proceedings of 36th IEEE PESC, Recife, Brazil, pp. 861–866 (2005)
11. Holtz, J., and Oikonomou, N.: Neutral point potential balancing algorithm at low modulation index for three-level inverter medium voltage drives. In: IEEE Transactions on Industrial Applications, vol. 43, no. 3, pp. 761–768 (2007)
12. Park, J.-J., Kim, T.-J., and Hyun, D.-S.: Study of neutral point potential variation for three-level NPC inverter under fault condition. In: Proc. 34<sup>th</sup> IEEE IECON, pp. 983–988 (2008)
13. Ceballos, S., Pou, J., Robles, E., Gabiola, I., Zaragoza, J., Villate, J.L., and Boroyevich, D.: Three-level converter topologies with switch breakdown fault-tolerance capability. In: IEEE Transactions on Industrial Electronics, vol. 55, no. 3, pp. 982–995 (2008)
14. Li, S., and Xu, L.: Strategies of fault tolerant operation for three-level PWM inverters. In: IEEE Transactions on Industrial Electronics, vol. 21, no. 4, pp. 933–940 (2006)

15. Li, J., Huang, A.Q., Liang, Z., and Bhattacharya, S.: Analysis and Design of Active NPC (ANPC) Inverters for Fault Tolerant Operation of High-Power Electrical Drives. In: IEEE Transactions on Industrial Electronics, vol. 27, pp. 519–533 (2012)
16. Ceballos, S., Pou, J., Robles, E., Zaragoza, J., and Martin, J.L.: Performance evaluation of fault-tolerant neutral-point-clamped converters. In: IEEE Transactions on Industrial Electronics, vol. 57, no. 8, pp. 2709–2718 (2010)
17. Wu, B.: High-Power Converters and AC Drives. IEEE Press/John Wiley & Sons Interscience, New Jersey (2006).